NeuroImage 264 (2022) 119748

Contents lists available at ScienceDirect

NeuroImage

journal homepage: www.elsevier.com/locate/neuroimage

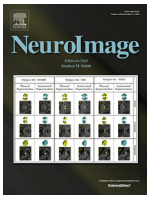

The thalamocortical inhibitory network controls human conscious perception

Jeehye Seo[a,1], Dae-Jin Kim[b,1], Sang-Han Choi[a], Hyoungkyu Kim[a], Byoung-Kyong Min[a,c,*]

[a] Institute for Brain and Cognitive Engineering, Korea University, Seoul 02841, Korea
[b] Department of Psychological and Brain Sciences, Indiana University, Bloomington, IN 47405, United States of America
[c] Department of Brain and Cognitive Engineering, Korea University, Seoul 02841, Korea

ARTICLE INFO

Keywords:
Conscious perception
Default-mode network
Illusory colour
Thalamocortical inhibitory network
Thalamic reticular nucleus

ABSTRACT

Although conscious perception is a fundamental cognitive function, its neural correlates remain unclear. It remains debatable whether thalamocortical interactions play a decisive role in conscious perception. To clarify this, we used functional magnetic resonance imaging (fMRI) where flickering red and green visual cues could be perceived either as a non-fused colour or fused colour. Here we show significantly differentiated fMRI neurodynamics only in higher-order thalamocortical regions, compared with first-order thalamocortical regions. Anticorrelated neurodynamic behaviours were observed between the visual stream network and default-mode network. Its dynamic causal modelling consistently provided compelling evidence for the involvement of higher-order thalamocortical iterative integration during conscious perception of fused colour, while inhibitory control was revealed during the non-fusion condition. Taken together with our recent magnetoencephalography study, our fMRI findings corroborate a thalamocortical inhibitory model for consciousness, where both thalamic inhibitory regulation and integrative signal iterations across higher-order thalamocortical regions are essential for conscious perception.

1. eTOC blurb

Thalamocortical temporal dynamics was differentiated particularly in the higher-order visual processing stage between illusory (fused) colour perception and physically presented (non-fused) colour perception. DMN activity was disinhibited during illusory perception. Both MEG and fMRI studies provide corroborating evidence for thalamocortical inhibitory control and integrative signal iterations during human conscious perception.

2. Introduction

The experience of conscious perception is essential to everyday life, but the neural signatures underlying this process remain unclear. Recently, we performed a visual flickering experiment to examine the role of thalamocortical interactions in conscious perception using magnetoencephalography (MEG) (Min et al., 2020). In a comparison between (physically existing) individual red/green colours and their illusory fused orange colour, we observed thalamocortical inhibitory coupling between the thalamus and visual cortex during conscious perception and provided experimental (Min et al., 2020) and theoretical (Min, 2010) evidence that the thalamocortical inhibitory network is a gateway to conscious mental representations. However, the significance of thalamocortical networking in conscious perception will be further corroborated if these observations are verified using other neuroimaging modalities with higher spatial resolution such as functional magnetic resonance imaging (fMRI).

It has been suggested that conscious perception may be accomplished via iterative and integrative communications across modal-specific individual thalamic subdivisions and their corresponding cortices (Min, 2010). There generally are two types of thalamic relay nuclei, *i.e.* first-order and higher-order thalamic relay nuclei (Sherman, 2016), and they have been reported to exhibit different firing-mode behaviours (Ramcharan et al., 2005). More bursting occurs in higher-order relays than in first-order relays. Min (2010) proposed that conscious perception could be accomplished and elaborated through integrative processing across the first-order input signal and higher-order signals from its functionally associated cortices throughout the latticework structure of the thalamic reticular nucleus (TRN), through which major inhibitory control over the thalamic relay nuclei is performed. For example, the lateral geniculate nucleus (LGN) and pulvinar respectively comprise the first- and higher-order thalamic relay cells in visual processing.

* Corresponding author.
E-mail address: min_bk@korea.ac.kr (B.-K. Min).
[1] These authors contributed equally to this work.

https://doi.org/10.1016/j.neuroimage.2022.119748.
Received 30 September 2022; Received in revised form 7 November 2022; Accepted 8 November 2022
Available online 9 November 2022.

Conscious perception becomes more refined as the higher-order relay signals run cumulatively through the relevant thalamocortical loops. Signal iterations during conscious perception could be examined using the neurodynamic causal trajectory of fMRI signals across higher-order thalamic relay nuclei (*e.g.* pulvinar) (Sherman, 2016) and their corresponding visual cortices for advanced processing (*e.g.* V2 and V4).

In addition, ongoing conscious experience has been studied in relation to the default-mode network (DMN) (Smallwood et al., 2021; Sormaz et al., 2018; Stawarczyk et al., 2011). In a recent report regarding the alternating change between the internal and external modes of conscious states (Kim et al., 2021), the internal mode was reported to be related to higher internal information-sharing amongst brain regions, as reflected in a synchronised brain network, and co-activation pattern analysis of the internal state revealed its correlation with the DMN. Presently, the known roles of the DMN include automated information processing (Vatansever et al., 2017), naturalistic perception (Brandman et al., 2021), self-referential processing (Raichle et al., 2001), and self-reflective thinking (Gusnard et al., 2001). All these observations imply the significance of the DMN in building and updating internal models of the world during conscious perception (Ramírez-Barrantes et al., 2019). Thus, compared with perception of the physically existing colours, red and green, forming the internal representation of a mentally fused colour appears to be associated with marked changes in DMN activity. Taken together, in this study, using the same experimental stimuli as in our previous MEG study (Min et al., 2020), we investigated neurodynamic changes in fMRI signals in the thalamocortical network as well as in the DMN during conscious perception of illusory mental representation. We hypothesised that inhibitory control of higher-order thalamic regions to the related cortical activation in the visual stream network (VSN) and DMN would play a pivotal role to differentiating conscious perception between fusion and non-fusion conditions, reflected in different neurodynamics of their blood-oxygen-level-dependant (BOLD) signals.

3. Materials and methods

3.1. Participants

Thirty-nine healthy volunteers (age: 23.5 ± 2.0 years; 21 men and 18 women) participated in this study. All participants had normal or corrected-to-normal vision, and none was colour-blind as determined by the *Ishihara* colour test. All participants were free of neurological and psychiatric illnesses, any contraindications for magnetic resonance imaging (MRI) scanning, current and past alcohol/drug abuse or dependence, and current use of illicit substances. All participants provided written informed consent and received payment for their participation. The study was conducted in accordance with the ethical guidelines established by the Institutional Review Board of Korea University (No. KUIRB-2021–0218–01) and the Declaration of Helsinki (World Medical Association, 2013).

3.2. Materials and procedure

A 5 × 5 LED array of 3-mm round diffused bicolour (red and green) light emitting diode (LED) lamps (model number: 100F3W-YT-REGR-CA, Chanzon Technology) was used to present the stimuli (Min et al., 2020). As shown in Fig. S1, five rows and columns of an LED grid in this array were lit on a black panel, and the gap between two adjacent rows or columns was 1 cm. The wavelengths for the red and green LEDs were 620–625 nm and 515–520 nm, respectively. These wavelengths are relevant for the stimulation of human retinal long-wave and middle-wave photoreceptors exhibiting optimal responses to the colours red and green, respectively, as their mean absorbance wavelengths are 562.8 nm and 533.8 nm for red and green, respectively (Bowmaker and Dartnall, 1980). According to the CIE 1931 RGB colour matching functions (CIE, 1931), the maximal peak of the monochromatic test was detected at approximately 610 nm for red and 540 nm for green. To avoid possible confounding luminance effects, the luminous intensity was balanced across these two colours to the extent possible, in both a psychometric and a physical (approximately 800 mcd) manner. To ensure that the light was evenly distributed, a thin plastic diffuser was positioned over the LED array.

The experimental paradigm was employed from our previous MEG study (Min et al., 2020) to investigate neurodynamic changes in BOLD signals in the thalamocortical visual perception network. Amongst the different types of presentation times used in our previous MEG study (Min et al., 2020), the present functional MRI (fMRI) study employed the 50-ms flickering condition because the same physical (bottom-up) stimulation of the 50-ms presentation condition occasionally yielded different subjective perceptual (top-down) responses of either the fusion or non-fusion condition, which was thus optimal to investigate top-down aspects of conscious perception. In the 50-ms presentation condition, red and green LEDs were alternately lit with a 50 ms of their individual flickering time, and these flickered colour stimuli were presented for 5 s in each trial, with variable inter-trial intervals ranging from 6 s to 10 s (centred at 8 s). To avoid possible afterimage in the retina, a 5-ms empty presentation gap was inserted between two consecutive red and green stimuli. This gap may play a wash-out role for the previously presented colour stimulation on the retina, as the time courses of retinal afterimages are interrupted by the duration of the temporal gap (Di Lollo et al., 1988). The entire experiment consisted of two runs of fMRI scanning and a short break in-between. Forty trials of the 50-ms flickering condition were randomly presented within the two runs. Participants were instructed to press a button with their right or left index finger depending on whether they perceived a fused colour of orange or not, with the response hands counterbalanced across participants. To prevent movement artifacts, participants were instructed to press a button after the end of each 5-s flickering presentation. To obtain comparable fMRI signals across fusion and non-fusion conditions and to avoid bias in transient brain activity across the two discrete runs, depending on whether both fusion and non-fusion responses were detected within a run, the run exhibiting both responses was eventually selected for further analyses. If both runs exhibited both responses, the run with a more evenly distributed number of responses was selected. Consequently, the 50-ms flickering condition yielded both responses of fusion (65.6%) and non-fusion (34.4%) conditions.

3.3. fMRI acquisition

MR image acquisition was performed on a Siemens 3T MAGNETOM Trio Tim syngo scanner (Siemens Healthcare, Erlangen, Germany) using a 32-channel head coil. Before the experiment, participants received a detailed explanation of the experimental procedure and were familiarised with the experimental surroundings and stimuli. Participants were instructed to maintain their eyes open and gaze at the LED panel located outside the MRI shielding room through the mirror positioned on the head coil, with the LED light visible through an electromagnetic shielded window. The distance between the LED panel and the participants was approximately 180 cm, resulting in a visual angle of 2.88°. To maximise colour perception, darkness was maintained both inside and outside the MRI shielding room during the LED flickering experiment. Functional scans consisted of two successive runs, where fMRI data were collected using an echo-planar image sequence with removal of the first 5 vol (~10 s) resulting in a total of 650 vol (~21 min 40 s) [repetition time (TR) = 2 s; echo time (TE) = 30 ms; flip angle (FA) = 90°; multiband acceleration factor = 3; acquisition matrix = 96 × 96; field of view (FOV) = 192 × 192 mm^2; in-plane voxel size = 2 × 2 × 2 mm^3; 75 transverse slices; no slice gap]. Three-dimensional anatomical magnetisation prepared rapid acquisition gradient echo (MPRAGE) images were collected for each participant after fMRI data collection [TR = 2.3 s;

TE = 2.13 ms; inversion time (TI) = 0.9 s; FA = 9°; acquisition matrix = 256 × 256; in-plane voxel size = 1 × 1 × 1 mm^3; 224 sagittal slices].

3.4. Data analysis

3.4.1. fMRI pre-processing

Pre-processing was performed using SPM12 (https://www.fil.ion.ucl.ac.uk/spm/software/spm12) and MRIQC (https://www.mriqc.readthedocs.io). Functional scans were pre-processed with a standard task-based fMRI processing pipeline: slice-timing correction (using the first slice as the reference slice), motion correction, co-registration, grey/white matter segmentation, normalisation to the Montreal Neurological Institute (MNI) template, and spatial smoothing using an 8-mm full-width at half-maximum (FWHM) Gaussian kernel. Subsequently, potential head-motion effects were minimised with additional exclusion of highly moving participants if: (1) averaged head movement measured with frame-wise displacement (FD) was > 0.2 mm and (2) the percentage of volumes with high motion, defined as relative FD > 0.2 mm, was > 30%. Thus, the data of six participants were excluded from further analyses based on excessive head motion during the fMRI session.

3.4.2. General linear model (GLM) for fMRI analysis

Functional activation during the visual perception task was examined using a standard GLM pipeline of SPM12. For each participant, the fMRI design matrix fitting the entire flickering duration included stimulation and fixation conditions with six motion parameters, where we specified two response conditions (*i.e.* fusion and non-fusion) based on the participant's response to the 50-ms flickering stimuli. Contrasts of interest included 'fusion – fixation', 'non-fusion – fixation', and 'fusion – non-fusion', where the fixation condition was defined based on the interval between the subject's response onset and the next flickering onset. In the second level analyses, to detect the statistical significance of these contrasts, one-sample *t*-tests were performed for each within-condition (*i.e.* 'fusion – fixation' and 'non-fusion – fixation') and paired *t*-tests were conducted for the between-condition (*i.e.* 'fusion – non-fusion'). To correct for multiple comparisons, a permutation-based voxel-wise non-parametric test was performed using the threshold-free cluster enhancement (TFCE) toolbox (http://dbm.neuro.uni-jena.de/tfce) (Smith and Nichols, 2009). To report clusters of voxels significantly related to conscious perception of either fused or non-fused colour, we used a height threshold of TFCE $p < 0.001$ with an extent threshold of $k \geq 100$ for the within-condition (fusion and non-fusion) and a height threshold of TFCE $p < 0.05$ with an extent threshold of $k \geq 100$ for the between-condition (fusion – non-fusion; Fig. 1 and Table S1). Based on our previous finding of sustained thalamocortical interaction during conscious perception (Min et al., 2020), we subsequently investigated the temporal dynamics of fMRI time-series between the fusion and non-fusion conditions using an event-related GLM approach with a 1-s step. Functional activation, defined based on the beta weights from the GLM, was compared using two-sided paired *t*-tests for the same contrasts of interest of the 50-ms flickering condition.

Subsequently, to investigate task-relevant thalamocortical neurodynamics in both the visual stream network (VSN) and default-mode network (DMN), the following thalamocortical regions of interest (ROIs) were selected for further analyses: the lateral geniculate nucleus (LGN), pulvinar (PUL), medial dorsal nucleus of thalamus (MD), primary visual cortex (V1), secondary visual cortex (V2), V4, dorsolateral prefrontal cortex, anterior insular cortex, middle temporal gyrus, medial prefrontal cortex, posterior cingulate cortex, and angular gyrus. These ROIs included the significantly activated regions during the task together with the crucial regions for the VSN and DMN. Three thalamic ROIs (the LGN, PUL, and MD) were anatomically defined using the Wake Forest University Pick Atlas (https://www.nitrc.org/projects/wfu_pickatlas). The numbers of voxels within the right thalamic ROIs were 48 for LGN, 272 for pulvinar, and 127 for medial dorsal nucleus of thalamus, and 43, 281, and 117 within the left thalamic ROIs, respectively. The remaining cortical ROIs were defined as 5-mm radius spheres centred on the peak activations of the within- and between-conditions. Each of these ROIs plays a significant role for either the VSN or DMN. For example, V1 and V2 were analysed for striate and extrastriate visual processing and V4 was analysed because it is considered crucial for colour-perception (Bartels and Zeki, 2000). Beta weights were averaged separately within these 12 ROIs and extracted for further analyses (temporal dynamics) using the region of interest extraction toolbox (http://web.mit.edu/swg/software.htm). As similar dynamics were observed in the left hemisphere, all (sub)cortical activities were analysed from the right hemisphere.

3.4.3. Analysis of co-activated thalamocortical links

Based on the previous results of fMRI beta weights, the above 12 ROIs in both hemispheres were selected to investigate which connectivity across brain areas most highly contributed to the conscious perception of the mentally fused colour. To investigate the co-activated thalamocortical links during the visual perception task, the fMRI beta weights of the trials for the fusion and non-fusion conditions were individually averaged in each ROI. The averaged beta weights of each time window post-stimulus (per a 1-s step during the stimulus presentation) were compared with those of the stimulus onset time window (Fig. S2). The links were defined based on simultaneous increase (noted as a positive link) or decrease (noted as a negative link) of the fMRI beta weights at the same time across the corresponding two regions amongst all the ROIs.

$$Positive\ Link_{i_t j_t} = \begin{cases} 1, & \text{if } \beta_{i_t} > \beta_{i_0} \text{ and } \beta_{j_t} > \beta_{j_0} \\ 0, & \text{Otherwise} \end{cases} \quad (1)$$

$$Negative\ Link_{i_t j_t} = \begin{cases} 1, & \text{if } \beta_{i_t} < \beta_{i_0} \text{ and } \beta_{j_t} < \beta_{j_0} \\ 0, & \text{Otherwise} \end{cases} \quad (2)$$

where, β_{i_t} is an averaged beta weight of region i at the time point t, and β_{i_0} is an averaged beta weight of region i at the onset of stimulation. The links were calculated separately in the fusion and non-fusion trials, and the links of fusion and non-fusion trials were compared in each time point. The significance was calculated with one-way analysis of variance and post-hoc analysis with false discovery rate (FDR) correction. The graphic tool Circos (Krzywinski et al., 2009) was used for the display of nodes and links.

3.4.4. Dynamic causal modelling (DCM)

DCM analysis (Friston et al., 2003) was conducted to investigate the functional interaction across the core higher-order thalamocortical regions related to the conscious perception of fused or non-fused colour using DCM12.5 implemented in SPM12. We hypothesised that interaction effects of conscious perception across the higher-order thalamocortical network would be differentially modulated depending on whether either a fused colour or non-fused colour was perceived under the same 50-ms flickering stimulus condition. Based on the results of SPM analysis, we focused on the higher-order thalamocortical network for the core VSN, where the intercommunicative configuration of higher-order thalamic cells of the pulvinar and their corresponding extrastriate visual cortices (*i.e.* V2 and V4) was modelled with full bidirectional connections to describe possible neural interactions between them related to the conscious perception of fused or non-fused colour using the 50-ms flickering stimuli. Since LGN did not exhibit significantly different neurodynamics between fusion and non-fusion conditions (working simply for a primary relay station of visual input), it was not included in the DCM analysis. Therefore, as shown in Fig. 3, the pulvinar, V2, and V4 were mutually and bidirectionally connected and V1 was linked to V2 as visual stimulation input, which may be neurophysiologically plausible. To investigate thalamic reticular nucleus(TRN)-mediated thalamic inhibition during conscious perception (Min, 2010; Min et al., 2020), self-inhibition was additionally modelled into the pulvinar since the

TRN provides a major inhibitory input to thalamic cells (Pinault, 2004; Shu and McCormick, 2002). As the 2-s post-stimulus time window was observed as the most optimal for the present task performance (Fig. 2), the time series at the 2-s post-stimulus time window was extracted using the volume of interest module in SPM12 for the DCM analysis. Parameters of this model were estimated based on Bayesian model averaging (Zeidman et al., 2019) to compare between-condition differences in fusion and non-fusion perception, and the significance of connectivity was examined with a posterior probability of a 95% confidence interval. To investigate effective connections per task-relevant modulations, the positive (increase) and negative (decrease) values of endogenous baseline connections as well as modulatory effects across the pulvinar, V2, and V4 were statistically analysed for both the fusion and non-fusion conditions using FDR-corrected two-sided one-sample *t*-tests. The modulatory effects of both the fusion and non-fusion conditions were also compared using FDR-corrected two-sided paired *t*-tests.

4. Results

4.1. Thalamocortical functional activation

Functional activation of the fusion and non-fusion conditions was examined using a standard general linear model (GLM) pipeline of SPM12 (https://www.fil.ion.ucl.ac.uk/spm/software/spm12). Contrasts of interest included 'fusion – fixation', 'non-fusion – fixation', and 'fusion – non-fusion'. That is, 'fusion – fixation' and 'non-fusion – fixation' were within-condition contrasts, and their difference (fusion – non-fusion) was the between-condition contrast during 50-ms flickering stimulation, where the fixation condition was defined based on the interval between the subject's response onset and next flickering onset (mean ± SD: 6.90 ± 0.26 s). As shown in Fig. 1A and B and Table S1, the significantly activated brain regions of conscious perception for both fusion and non-fusion conditions involved the VSN (showing increased activation) including the LGN, pulvinar, medial dorsal nucleus of the thalamus (MD), visual cortices (V1, V2, and V4), and anterior insular cortex (AIC), as well as the DMN (showing decreased activation) including the middle temporal gyrus (MTG), posterior cingulate cortex (PCC), and medial prefrontal cortex (mPFC). Compared with the commonly activated regions of the VSN between the fusion and non-fusion conditions, DMN activation (particularly of the mPFC and PCC) was less suppressed for the fusion condition than for the non-fusion condition, resulting in enhanced activation (red blobs) of the mPFC and PCC in the fusion minus non-fusion condition (Fig. 1C and Table S1). Notably, functional activation of the thalamocortical VSN was obviously observed during conscious perception in both the fusion and non-fusion conditions. Differences in functional activation between fusion and non-fusion perception are also shown in Fig. 1C. Although task-relevant thalamic activation was clearly observed in both fusion and non-fusion conditions (Fig. 1A and B), this typical approach did not suffice to detect significant differences in thalamic activity when brain activation for non-fused colour perception was subtracted from that for fused colour perception (Fig. 1C). Table S1 shows the MNI coordinates of significantly activated brain regions for fusion and non-fusion and their differences in an fMRI block design.

4.2. Thalamocortical temporal neurodynamics

Presumably, task-dependant instantaneous (or negligible) differences in thalamic activation might not be detectable using a conventional fMRI block design. Thus, we additionally employed the event-related design in the present study, which appeared to be advantageous to shed light on revealing the slight differences in thalamocortical temporal neurodynamics between fusion and non-fusion conditions. To investigate task-relevant thalamocortical neurodynamics in both the VSN and DMN, the following 12 regions of interest (ROIs) were selected for an fMRI event-related design, including the significantly activated regions during the task (Fig. 1) together with the crucial regions for the VSN and DMN: LGN, pulvinar, MD, V1, V2, V4, MTG, PCC, angular gyrus, IC, mPFC, and dorsolateral prefrontal cortex. Notably, as shown

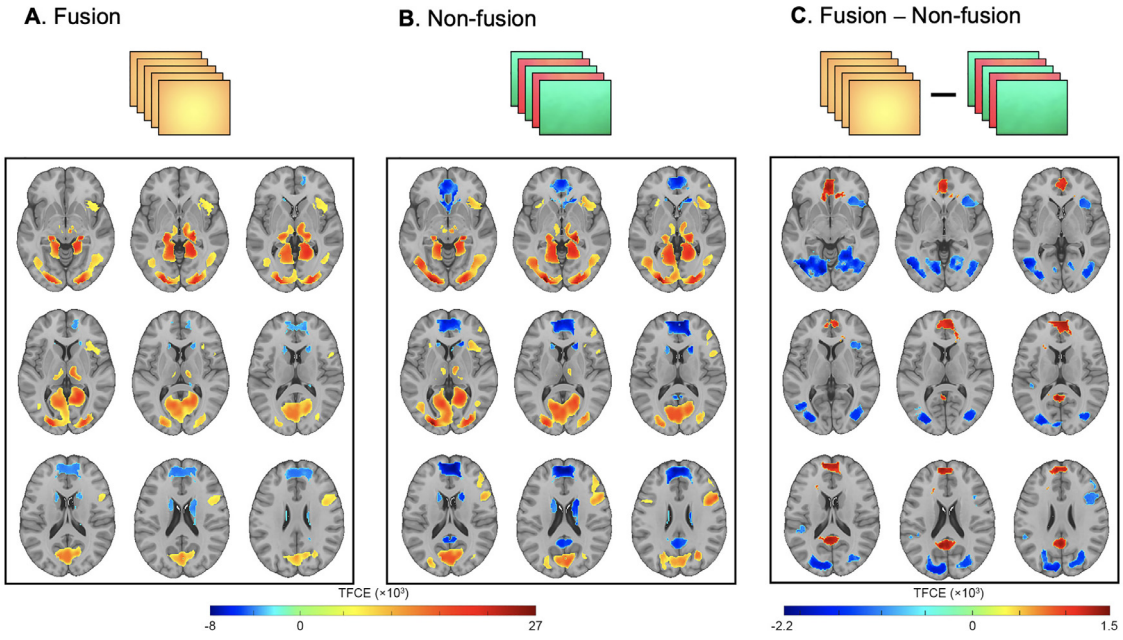

Fig. 1. Functional activation during the visual conscious perception task. Functional activation for (A) fusion and (B) non-fusion perception is displayed using within-condition contrasts from a random-effects GLM (TFCE FWE-corrected $p < 0.001$, $k \geq 100$). Note that thalamocortical activation during the fusion and non-fusion conditions was compared with fixation periods, where hot and cool colours represent increased and decreased task activity compared to fixation during visual perception processing, respectively. (C) Activation difference between fusion and non-fusion perception. Compared to the non-fusion condition, the fusion condition showed greater activation in the DMN (*i.e.* the mPFC, PCC, and left MTG; red clusters) and less activation in the VSN (*i.e.* V2, V4, the DLPFC, and the right AIC; blue clusters), respectively (TFCE FWE-corrected $p < 0.05$, $k \geq 100$). Axial slices are evenly spread from $z = -6$ to $z = 26$ in the MNI 152 template. *Abbreviations*. mPFC, medial prefrontal cortex; PCC, posterior cingulate cortex; MTG, middle temporal gyrus; DLPFC, dorsolateral prefrontal cortex; AIC, anterior insular cortex.

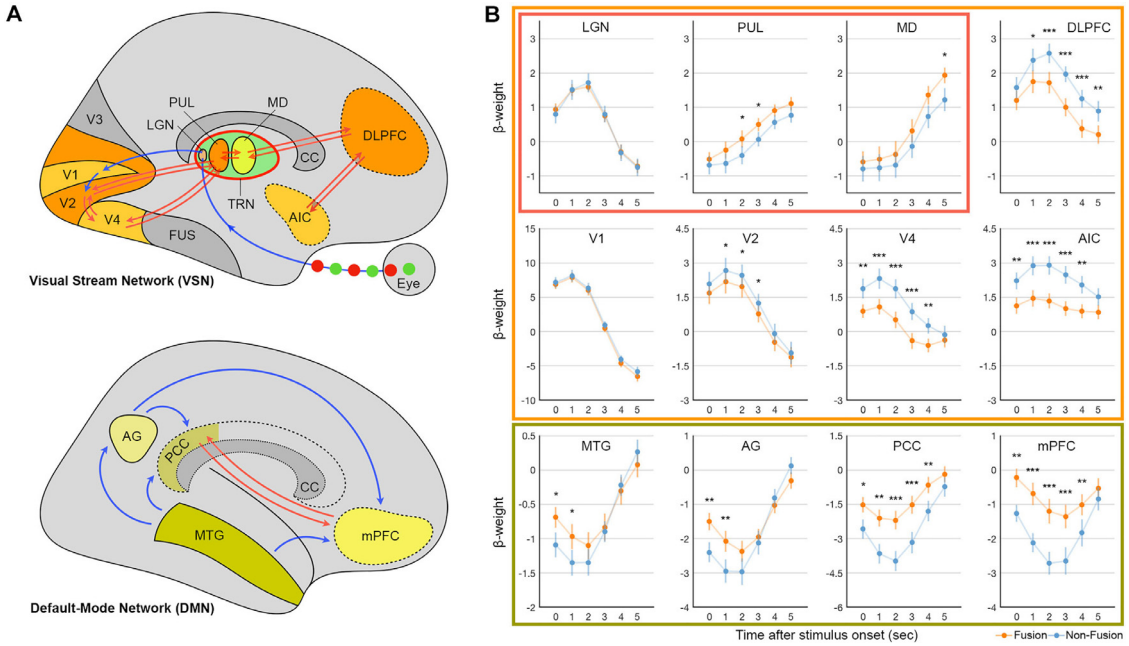

Fig. 2. Thalamocortical network and temporal dynamics of regional brain activity. (A) Schematic representation of the interactive relationship between the thalamocortical iterative visual stream network (VSN; top) and default-mode network (DMN; bottom). Note the higher-order processing networks (red arrows) yielding significant differences in brain activity between fusion and non-fusion perception (after 2-s post-stimulus). (B) Temporal dynamics of brain activity between the fusion (orange curves) and non-fusion (blue curves) conditions in 12 regions of interest as a function of time after visual stimulus onset. Beta weights were computed from the GLM of their BOLD signals. The red box highlights thalamic subdivisions, and the orange and green boxes indicate the VSN and DMN, respectively. All (sub)cortical activities derived from the right hemisphere, with similar dynamics observed in the left hemisphere (not shown). Error bars indicate standard errors of the mean; $N = 33$, $^{***}\ p < 0.001$, $^{**}\ p < 0.01$, and $^{*}\ p < 0.05$. *Abbreviations*. AG, angular gyrus; AIC, anterior insular cortex; CC, cingulate cortex; DLPFC, dorsolateral prefrontal cortex; FUS, fusiform gyrus; LGN, lateral geniculate nucleus; MD, medial dorsal nucleus of thalamus; mPFC, medial prefrontal cortex; MTG, middle temporal gyrus; PCC, posterior cingulate cortex; PUL, pulvinar; TRN, thalamic reticular nucleus; V1, primary visual cortex; V2, secondary visual cortex.

in Fig. 2B, the primary (first-order) thalamocortical regions such as the LGN and V1 exhibited no significant differences between the fusion and non-fusion conditions during the entire 5-s stimulation. However, the pulvinar (belonging to the higher-order visual thalamic nuclei) showed significant differences between the conditions at the 2-s post-stimulus (fusion 0.079, non-fusion −0.395; $t(32) = 2.63$, $p < 0.05$) and 3-s post-stimulus (fusion 0.496, non-fusion 0.072; $t(32) = 2.64$, $p < 0.05$) time windows. For higher-order visual cortical regions, V4 and the dorsolateral prefrontal cortex (DLPFC) in the VSN showed significant differences between the fusion and non-fusion conditions.

Importantly, cortical behaviours were inverted relative to thalamic behaviours between fusion and non-fusion perception. Cortical suppression in V2, V4, the AIC, and the DLPFC was temporally coupled with enhanced thalamic responses in the pulvinar and MD during the conscious perception of fused colour. That is, the higher-order thalamic subdivisions (*e.g.* the pulvinar and MD) showed higher activity for the fusion condition than for the non-fusion condition; this phenomenon was reversed in cortical regions such as V2, V4, the AIC, and the DLPFC. On the other hand, the brain regions of the DMN showed less suppressed activity for the fusion condition than for the non-fusion condition (see the green box in Fig. 2B; MTG, AG, PCC, and mPFC). Compared with the AIC, the posterior IC showed no significant differences between the conditions throughout the 5-s stimulation duration (not shown).

Taken together with our previous thalamic inhibitory networking model of consciousness (Min, 2010) and MEG observations (Min et al., 2020), a schematic signal networking is delineated in Fig. 2A, which indicates that a higher-order thalamocortical network (red arrows) plays a key role during conscious perception of fusion and non-fusion perception. For example, for the fusion condition, integrative signal iterations are involved across the pulvinar, V2, and V4. However, this cooperative signal looping was under inhibitory control for non-fusion perception (red arrows in Fig. 2A and Fig. 3C).

4.3. Thalamocortical dynamic causal relationship

The dynamic causal modelling (DCM) (Friston et al., 2003) of the core thalamocortical VSN and co-activated thalamocortical links of BOLD signals across 12 ROIs were analysed. At the 2-s post-stimulus time window when the most optimal conscious perception occurred based on the temporal neurodynamics of regional brain activity (Fig. 2B), the values of the modulatory effects in DCM across the pulvinar, V2, and V4 are displayed in Fig. 3. All endogenous baseline connectivity across these regions at the 2-s post-stimulus time window was significantly higher than zero ($p < 0.001$, false discovery rate (FDR)-corrected). Moreover, all modulatory effects across the pulvinar, V2, and V4 were significantly higher in the fusion condition than in the non-fusion condition ($p < 0.001$, FDR-corrected). Strikingly, there was significantly lower self-inhibition of the pulvinar in the fusion condition than in the non-fusion condition (fusion = -0.066×10^{-7} Hz; non-fusion = -0.0006×10^{-7} Hz; $t(32) = -9.01$, $p < 0.05$, FDR-corrected).

5. Discussion

This study aimed to provide haemodynamic evidence supporting the essential role of thalamic regulation during conscious perception in humans. The present fMRI observations, together with those of our recent MEG study (Min et al., 2020), provide corroborating evidence that higher-order thalamocortical inhibitory control and integrative signal iterations across the thalamocortical network are essential for conscious perception between fusion (illusory) and non-fusion mental representation. This study also revealed temporally sequential neurodynamic trajectories across first-order and higher-order thalamic nuclei (*e.g.* the LGN and pulvinar, respectively) and their corresponding visual cortices (*e.g.* V1 and the extrastriate visual cortices, respectively). Although this view was proposed by visual processing studies

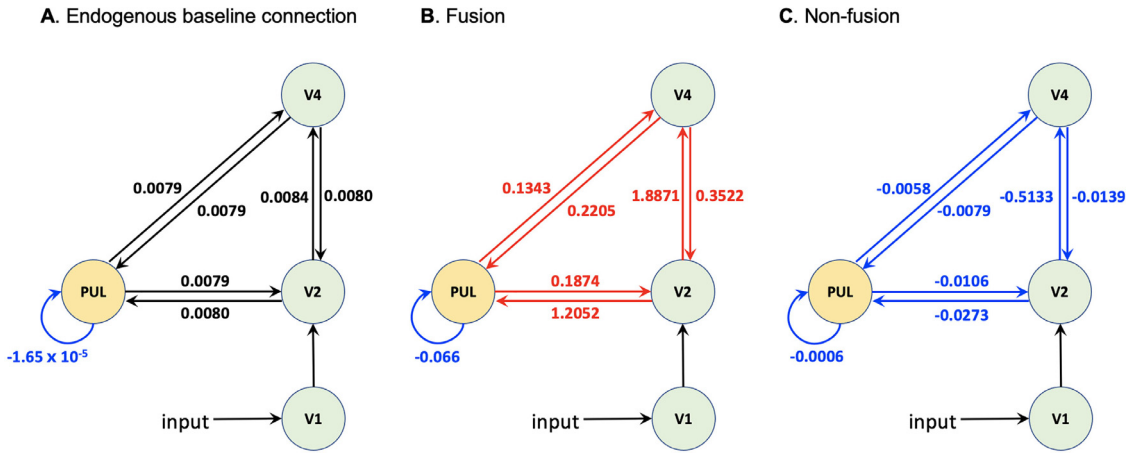

Fig. 3. Dynamic causal modelling (DCM) of fusion and non-fusion perception. DCMs were designed across representative higher-order thalamocortical regions consisting of the pulvinar (PUL), V2, and V4 with an input to V1 at the 2-s post-stimulus time window to examine the core thalamocortical visual stream network (VSN) during conscious perception. (A) Endogenous baseline connections (unit: Hz) are displayed across these core thalamocortical network of the VSN. Estimated connectivity parameters (*i.e.* modulatory effects) of (B) fusion and (C) non-fusion perception are shown across these regions, where positive values (red arrows) indicate connectivity excitation and negative values (blue arrows) indicate connectivity inhibition (the scaled values of the modulatory effect for the fusion and non-fusion conditions should be multiplied with the factor of 10^{-7}). Note the inhibitory connection (blue arrows) across the pulvinar, V2, and V4 during non-fusion perception compared with the excitatory connection (red arrows) during fusion perception.

(Nolte, 2009; Ramcharan et al., 2005), and Min (2010) hypothesised that signal looping dynamics are necessary for the accomplishment of conscious perception, this may be the first study to empirically demonstrate the phenomenon using fMRI neuroimaging during human conscious perception.

5.1. Temporally sequential neurodynamics

As shown in Fig. 2B, the significantly different neurodynamic behaviours of brain activity in conscious perception between the (illusory) fusion and (physically presented) non-fusion conditions were observed and reflected in the temporally sequential neurophysiological patterns of brain activity. Notably, there were no significant differences between the fusion and non-fusion conditions in the first-order thalamic (*i.e.* the LGN) and cortical (*i.e.* V1) visual processing stages, but their differences became obvious as their signals progressed to higher-order thalamic (*i.e.* the pulvinar) and cortical (*i.e.* from V2 to its downstream destination) visual processing stages. These observations are plausible in the sense that the primary visual processing stage (*i.e.* involving the LGN and V1) may simply receive and relay sensory inputs of consecutively presented red or green colours and would not be involved in the differentiating process between fusion and non-fusion perception, which may be initiated at a further hierarchical level of visual processing such as the higher-order thalamic (*e.g.* the pulvinar) and extrastriate visual cortices (*e.g.* V2 and V4). We observed significantly higher pulvinar activity during fusion perception than during non-fusion perception in the 2-s and 3-s post-stimulus time windows (Fig. 2B). Moreover, the consecutive 4-s and 5-s post-stimulus time windows exhibited significantly (marginally significant for the 4-s post-stimulus time window) different activity between these conditions in the MD, which is anatomically connected to the PFC (Behrens et al., 2003; Zhang et al., 2010). These observations appeared neurophysiologically plausible in terms of the temporal consequences of visual information processing. That is, the visual information of alternatively presented red and green colours was delivered first to V1 via the LGN, and these signals were fed back to the pulvinar. As the pulvinar plays a thalamic role of advanced visual information processing (Arcaro et al., 2015; Barron et al., 2015), the elaborated visual signals in the pulvinar may propagate to higher-order visual processing cortices such as V2 and V4. Consistently, a study on monkeys reported that the pulvinar controls information transmission between cortical regions (*i.e.* V4 and the temporo-occipital area) based on attention demands (Saalmann et al., 2012). Presumably, during the signal iterations across the first-order and higher-order visual processing stages in this study, the different neurodynamic behaviours of thalamic signals between the fusion and non-fusion conditions, initiating from the pulvinar and propagating to the MD, were eventually reflected in the PFC (downstream of the VSN).

5.2. Thalamocortical signal looping

Furthermore, the DCM results support the iterative integration of thalamocortical signals during fusion perception. As shown in Fig. 3B, cooperative signal iterations across higher-order thalamic (*e.g.* the pulvinar) and cortical (*e.g.* V2 and V4) areas were detected during the fusion perception of sequentially presented red and green stimuli. Presumably, when consecutive inputs of both colours are deemed a joint perception unit, the higher-order thalamocortical network appeared to be harmoniously involved in the colour-fusion process through stimulus-driven oscillations. These findings are in accordance with the importance of thalamocortical signal iterations in conscious perception of mental representation (Min, 2010). Conscious perception may be accomplished through sufficient signal iterations between individual thalamic modal-specific subdivisions and their corresponding modal cortices. This notion is consistent with previous findings of conscious access seemingly being characterised by entry of the perceived stimulus into a series of additional brain processes (Salti et al., 2015). For example, visual information can be further elaborated in terms of conscious awareness when that information moves iteratively back and forth between the thalamus and visual cortices. It is likely that the first-order thalamic relay cells in the LGN receive their driving afferents from ascending pathways and firstly send these signals to their corresponding V1, while higher-order thalamic relay cells cumulatively elaborate the information throughout the signal iterations within the thalamocortical looping network (Min et al., 2020). Consistently, robust enhanced activation of higher-order thalamic cells (*e.g.* in the pulvinar and MD), temporally coupled with suppressed haemodynamic responses of the corresponding cortices (*e.g.* V2, V4, the AIC, and the DLPFC; Fig. 2B), was observed during the perception of a fused colour, implicating the thalamus in the fusion process of two different incoming stimuli. Here, signal iterations between the cortices and thalamus may have generated the illusory colour perception of orange, although there was no physical orange input to the eyes.

5.3. Thalamocortical inhibitory control

Meanwhile, the DCM results revealed inhibitory control across the pulvinar, V2, and V4 for the individual perception of each red or green colour (Fig. 3). Consistently, as shown in Fig. 2B, the neurodynamic activity of the higher-order visual cortices such as V2, V4, and the DLPFC was higher in the non-fusion condition than in the fusion condition. Critically, the neurodynamic activity of the higher-order thalamic subdivisions such as the pulvinar and MD simultaneously exhibited reversed patterns. That is, cortical suppression in V2, V4, the AIC, and the DLPFC was temporally coupled with enhanced thalamic responses in the pulvinar and MD during conscious perception of the fused colour. This inverse relationship of brain activity between the thalamic subdivisions and their corresponding cortices was also observed in our previous MEG study (Min et al., 2020). A principal function of the thalamus is to inhibit cortical activation during the resting state (Halassa and Acsady, 2016; Poulet et al., 2012), and as a result, cortical excitation is possible only when the thalamus releases the cortex from the default inhibited state; for example, motor-related thalamic inhibition needs to be suppressed for motor cortical function activation (Deniau and Chevalier, 1985). Such thalamic disinhibition (or gating) may play a similar role in the conscious perception of mental representations. Thalamic disinhibition may trigger cortical excitation in the visual cortices generating differences in perception between fusion and non-fusion conditions. As shown in Fig. 3B, significantly lower self-inhibition of the pulvinar was observed in the fusion condition than in the non-fusion condition. This observation implies the substantial involvement of TRN-based thalamic disinhibition during conscious perception of the mentally fused illusory orange colour. As the TRN primarily contributes to inhibitory feedback control of the thalamocortical neurons (Lopes da Silva, 1991; Shu and McCormick, 2002), these observations consistently support the TRN-mediated thalamocortical inhibitory control model for conscious perception (Min, 2010). Based on their anatomical connections, the inhibitory TRN cells play a key role in coordinating conscious perception through the inhibitory feedback network across both the thalamus and cortex (Min, 2010). Throughout the latticework structure of the TRN, conscious perception could be established and refined through accumulating intercommunicative processing across the first-order input signal and higher-order signals over the relevant thalamocortical loops.

It has been reported that other structures outside of the thalamus, including the superficial superior colliculus (Basso and May 2017), the ascending arousal system (Munn et al., 2021), and numerous inhibitory structures (Halassa and Acsady, 2016), likely play crucial roles in conscious visual perception. The present thalamic inhibitory model in conscious perception is compatible with these previous studies since these extrathalamic structures contribute individually and locally to a temporally and spatially harmonious integration of each process in conscious perception, thus it does not necessarily conflict neurophysiologically with thalamic processing. Rather, both thalamic and extrathalamic processes seem to cooperate for an ultimate achievement of unitary conscious perception under a concerted unifying framework in different temporal neurodynamics and spatial focality, which would be a research topic for future study.

5.4. Significance of the default-mode network

Inversed activation between the fusion and non-fusion conditions across the visual processing stream (including V2, V4, the AIC, and the DLPFC) and in the DMN (*e.g.* the MTG, AG, PCC, and mPFC) was observed, and the activation of higher-order thalamic subdivisions resembled the DMN activation patterns (Fig. 2B). Based on the DLPFC–thalamus functional connectivity (Helm et al., 2018; Salomons et al., 2014) (Fig. S2) and control role of the AIC on the DMN (Chand and Dhamala, 2016; Sridharan et al., 2008), it is highly likely that the thalamocortical signalling from the visual processing stream to the DMN via TRN-mediated thalamocortical inhibitory control served to consciously perceive the mental representation, within which the activation patterns between the (illusory) fused colour and (physically presented) non-fused colour conditions showed significantly different behaviours.

The alternating change in conscious perception (fusion or non-fusion) via thalamocortical inhibitory control can be related to alternating activation between specific functional brain networks (*e.g.* the DMN and VSN). Our findings reinforced the importance of the DMN for conscious perception, particularly for the mental representation of illusory (fusion) perception. Higher neurodynamic activity of the DMN was observed during fusion perception, *i.e.* subjective imagery experience, than during non-fusion perception (the green box in Fig. 2B). The essential role of the DMN as a modality-independent core mental imagery network has been consistently reported (Daselaar et al., 2010; Zhang et al., 2018b). It has been suggested that visual illusions can be due to increased engagement of the DMN with the primary visual system (Shine et al., 2015). As shown in Fig. 2B, the temporal neurodynamics of DMN brain regions (*i.e.* the MTG, AG, PCC, and mPFC) behaved in a similar manner. That is, less suppressed activity was harmoniously observed across these DMN regions during the fusion condition than during the non-fusion condition. Such concordant behaviour within the DMN regions is a well-known characteristic of the DMN. For example, most studies on DCM-based DMN connectivity have indicated strong effective connectivity between mPFC and PCC areas (Di and Biswal, 2014; Sharaev et al., 2016). Furthermore, the temporal dynamic changes in brain activity (Fig. 2B) exhibited a reciprocal relationship between the DMN and VSN along with the visual processing stream during conscious perception.

Importantly, the anterior, not posterior, IC showed significantly different neurodynamics between the fusion and non-fusion conditions (Fig. 2B). Interestingly, core DMN regions are anticorrelated with the dorsal AI (dAI) and dorsal anterior cingulate cortex (dACC) (Chang and Glover, 2009; Fox et al., 2005). Reportedly, the insula is a multimodal integration region providing an interface between external information and internal motivational states (Craig, 2009; Seeley et al., 2007). The dAI and dACC were found to be functionally connected to a set of regions described as a decision-making and cognitive control network (Dosenbach et al., 2007; Grinband et al., 2006). Compared with the posterior insular, it has been suggested that the anti-correlation pattern between the DMN and central-executive network is modulated by an AI-based network, which primarily comprises the AI and dACC (Chand and Dhamala, 2016; Sridharan et al., 2008) as well as neural correlates of consciousness (Craig, 2009; Zhang et al., 2018a). For instance, the AI is involved in a wide range of cognitive processes, including switching between cognitive resources (Uddin and Menon, 2009) and reorienting attention (Ullsperger et al., 2010). Thus, the AI may have been consistently implicated in switching the dominant processing network between the VSN and DMN in this study.

5.5. Conclusion

Taken together, based on the coupled thalamocortical neurodynamics examined in this study, the thalamus appears to be playing a regulatory role over the entire system of thalamocortical loops as a dynamic core in conscious experience. Thus, the cognitive thalamus serves as a gateway to mental representation (Wolff and Vann, 2019). The inversed activation relationship between the higher-order thalamic regions and extrastriate visual cortices may be regulated through thalamic inhibitory control. This could consistently support the notion that TRN-centred thalamocortical inhibitory networking is involved in conscious perception. Thus, our present observations may provide neurophysiological haemodynamic evidence supporting the thalamic reticular networking model of consciousness in humans (Min, 2010). As the conscious perception of fused colour comprised an illusory mental representation, our present results support that TRN-mediated thalamocortical inhibitory networking is crucial for human conscious perception, even perception of non-tangible experiences (Min et al., 2020). This may be informative in terms

of the identity of human consciousness because conscious perception of mental representation can be achieved without external or physical stimulation. Although our MEG and fMRI studies together provided corroborating support for the importance of thalamocortical inhibitory control in conscious perception under the current human neuroimaging technical limitations, a series of invasive or non-invasive neuromodulatory experiments could additionally provide more convincing evidence for the TRN-centred thalamocortical inhibitory neurodynamic signature of human consciousness.

Author contributions

B.-K.M. conceived and designed the red-green alternating LED paradigm to investigate the thalamocortical networking for conscious perception of fusion colour, performed research, and wrote the main manuscript text. B.-K.M. and J.S. performed the fMRI experiment. B.-K.M., J.S., D.-J.K., S.-H.C., and H.K. analysed data and reviewed the manuscript.

Data and code availability

The MRI data is not publicly available because of data protection regulations. However, if a formal data sharing agreement is made, access can be provided in accordance with our Data Use and Access Policy. The analysis codes have been made publicly available on Github (https://github.com/cogmind1/2022NI_code).

Acknowledgements

We thank Dr. Peter Zeidman, Dr. Hae-Jeong Park, and Dr. Huijin Song for their valuable comments and analytic discussion. We are also thankful to Eul-Seok Hong and Jechoon Park for their kind assistance during the data acquisition and analysis. This work was supported by the Convergent Technology R&D Program for Human Augmentation (grant number 2020M3C1B8081319 to B.-K.M.), which is funded by the Korean government through the National Research Foundation of Korea. The authors declare no competing interests.

Supplementary materials

Supplementary material associated with this article can be found, in the online version, at doi:10.1016/j.neuroimage.2022.119748.

References

Arcaro, M.J., Pinsk, M.A., Kastner, S., 2015. The anatomical and functional organization of the human visual pulvinar. J. Neurosci. 35, 9848–9871.
Barron, D.S., Eickhoff, S.B., Clos, M., Fox, P.T., 2015. Human pulvinar functional organization and connectivity. Hum. Brain Mapp. 36, 2417–2431.
Bartels, A., Zeki, S., 2000. The architecture of the colour centre in the human visual brain: new results and a review. Eur. J. Neurosci. 12, 172–193.
Basso, M.A., May, P.J., 2017. Circuits for action and cognition: a view from the superior colliculus. Ann. Rev. Vision Sci. 3, 197.
Behrens, T.E.J., Johansen-Berg, H., Woolrich, M.W., Smith, S.M., Wheeler-Kingshott, C.A.M., Boulby, P.A., Barker, G.J., Sillery, E.L., Sheehan, K., Ciccarelli, O., Thompson, A.J., Brady, J.M., Matthews, P.M., 2003. Non-invasive mapping of connections between human thalamus and cortex using diffusion imaging. Nat. Neurosci. 6, 750–757.
Bowmaker, J.K., Dartnall, H.J., 1980. Visual pigments of rods and cones in a human retina. J. Physiol. 298, 501–511.
Brandman, T., Malach, R., Simony, E., 2021. The surprising role of the default mode network in naturalistic perception. Commun. Biol. 4, 79.
Chand, G.B., Dhamala, M., 2016. Interactions among the brain default-mode, salience, and central-executive networks during perceptual decision-making of moving dots. Brain Connect 6, 249–254.
Chang, C., Glover, G.H., 2009. Effects of model-based physiological noise correction on default mode network anti-correlations and correlations. Neuroimage 47, 1448–1459.
CIE, 1931. Proceedings of the Commission Internationale de l'Éclairage Proceedings. Cambridge University Press, Cambridge, UK.
Craig, A.D., 2009. How do you feel—now? The anterior insula and human awareness. Nature Rev. Neurosci. 10, 59–70.
Daselaar, S.M., Porat, Y., Huijbers, W., Pennartz, C.M., 2010. Modality-specific and modality-independent components of the human imagery system. Neuroimage 52, 677–685.
Deniau, J.M., Chevalier, G., 1985. Disinhibition as a basic process in the expression of striatal functions .2. The striato-nigral influence on thalamocortical cells of the ventromedial thalamic nucleus. Brain Res. 334, 227–233.
Di Lollo, V., Clark, C.D., Hogben, J.H., 1988. Separating visible persistence from retinal afterimages. Percept. Psychophys. 44, 363–368.
Di, X., Biswal, B.B., 2014. Identifying the default mode network structure using dynamic causal modeling on resting-state functional magnetic resonance imaging. Neuroimage 86, 53–59.
Dosenbach, N.U., Fair, D.A., Miezin, F.M., Cohen, A.L., Wenger, K.K., Dosenbach, R.A., Fox, M.D., Snyder, A.Z., Vincent, J.L., Raichle, M.E., 2007. Distinct brain networks for adaptive and stable task control in humans. Proc. Natl. Acad. Sci. 104, 11073–11078.
Fox, M.D., Snyder, A.Z., Vincent, J.L., Corbetta, M., Van Essen, D.C., Raichle, M.E., 2005. The human brain is intrinsically organized into dynamic, anticorrelated functional networks. Proc. Natl. Acad. Sci. 102, 9673–9678.
Friston, K.J., Harrison, L., Penny, W., 2003. Dynamic causal modelling. Neuroimage 19, 1273–1302.
Grinband, J., Hirsch, J., Ferrera, V.P., 2006. A neural representation of categorization uncertainty in the human brain. Neuron 49, 757–763.
Gusnard, D.A., Akbudak, E., Shulman, G.L., Raichle, M.E., 2001. Medial prefrontal cortex and self-referential mental activity: relation to a default mode of brain function. Proc. Natl. Acad. Sci. 98, 4259–4264.
Halassa, M.M., Acsady, L., 2016. Thalamic inhibition: diverse sources, diverse scales. Trends Neurosci. 39, 680–693.
Helm, K., Viol, K., Weiger, T.M., Tass, P.A., Grefkes, C., Del Monte, D., Schiepek, G., 2018. Neuronal connectivity in major depressive disorder: a systematic review. Neuropsychiatr. Dis. Treat..
Kim, M., Kim, H., Huang, Z., Mashour, G.A., Jordan, D., Ilg, R., Lee, U., 2021. Criticality creates a functional platform for network transitions between internal and external processing modes in the human brain. Front. Syst. Neurosci. 15.
Krzywinski, M., Schein, J., Birol, I., Connors, J., Gascoyne, R., Horsman, D., Jones, S.J., Marra, M.A., 2009. Circos: an information aesthetic for comparative genomics. Genome Res. 19, 1639–1645.
Lopes da Silva, F., 1991. Neural mechanisms underlying brain waves: from neural membranes to networks. Electroencephalogr. Clin. Neurophysiol. 79, 81–93.
Min, B.-K., 2010. A thalamic reticular networking model of consciousness. Theor. Biol. Med. Model 7, 10.
Min, B.K., Kim, H.S., Pinotsis, D.A., Pantazis, D., 2020. Thalamocortical inhibitory dynamics support conscious perception. Neuroimage 220, 117066.
Munn, B.R., Müller, E.J., Wainstein, G., Shine, J.M., 2021. The ascending arousal system shapes neural dynamics to mediate awareness of cognitive states. Nat. Commun. 12, 1–9.
Nolte, J., 2009. The Human Brain : an Introduction to Its Functional Anatomy, 6th ed. Mosby/Elsevier, Philadelphia, PA.
Pinault, D., 2004. The thalamic reticular nucleus: structure, function and concept. Brain Res. Rev. 46, 1–31.
Poulet, J.F.A., Fernandez, L.M.J., Crochet, S., Petersen, C.C.H., 2012. Thalamic control of cortical states. Nat. Neurosci. 15, 370–372.
Raichle, M.E., MacLeod, A.M., Snyder, A.Z., Powers, W.J., Gusnard, D.A., Shulman, G.L., 2001. A default mode of brain function. Proc. Natl. Acad. Sci. 98, 676–682.
Ramcharan, E., Gnadt, J., Sherman, S., 2005a. Higher-order thalamic relays burst more than first-order relays. Proc. Natl. Acad. Sci. 102, 12236–12241.
Ramírez-Barrantes, R., Arancibia, M., Stojanova, J., Aspé-Sánchez, M., Córdova, C., Henríquez-Ch, R.A., 2019. Default mode network, meditation, and age-associated brain changes: what can we learn from the impact of mental training on well-being as a psychotherapeutic approach? Neural Plast. 2019, 7067592.
Saalmann, Y.B., Pinsk, M.A., Wang, L., Li, X., Kastner, S., 2012. The pulvinar regulates information transmission between cortical areas based on attention demands. Science 337, 753–756.
Salomons, T.V., Dunlop, K., Kennedy, S.H., Flint, A., Geraci, J., Giacobbe, P., Downar, J., 2014. Resting-state cortico-thalamic-striatal connectivity predicts response to dorsomedial prefrontal rTMS in major depressive disorder. Neuropsychopharmacology 39, 488–498.
Salti, M., Monto, S., Charles, L., King, J.R., Parkkonen, L., Dehaene, S., 2015. Distinct cortical codes and temporal dynamics for conscious and unconscious percepts. Elife 4.
Seeley, W.W., Menon, V., Schatzberg, A.F., Keller, J., Glover, G.H., Kenna, H., Reiss, A.L., Greicius, M.D., 2007. Dissociable intrinsic connectivity networks for salience processing and executive control. J. Neurosci. 27, 2349–2356.
Sharaev, M.G., Zavyalova, V.V., Ushakov, V.L., Kartashov, S.I., Velichkovsky, B.M., 2016. Effective connectivity within the default mode network: dynamic causal modeling of resting-state fMRI data. Front. Hum. Neurosci. 10, 14.
Sherman, S.M., 2016. Thalamus plays a central role in ongoing cortical functioning. Nat. Neurosci. 19, 533–541.
Shine, J.M., Muller, A.J., O'Callaghan, C., Hornberger, M., Halliday, G.M., Lewis, S.J.G., 2015. Abnormal connectivity between the default mode and the visual system underlies the manifestation of visual hallucinations in Parkinson's disease: a task-based fMRI study. NPJ Parkinson's Disease 1, 15003.
Shu, Y.S., McCormick, D.A., 2002. Inhibitory interactions between ferret thalamic reticular neurons. J. Neurophysiol. 87, 2571–2576.
Smallwood, J., Turnbull, A., Wang, H.T., Ho, N.S.P., Poerio, G.L., Karapanagiotidis, T., Konu, D., Mckeown, B., Zhang, M.C., Murphy, C., Vatansever, D., Bzdok, D., Konishi, M., Leech, R., Seli, P., Schooler, J.W., Bernhardt, B., Margulies, D.S., Jefferies, E., 2021. The neural correlates of ongoing conscious thought. iScience 24.

Smith, S.M., Nichols, T.E., 2009. Threshold-free cluster enhancement: addressing problems of smoothing, threshold dependence and localisation in cluster inference. Neuroimage 44, 83–98.
Sormaz, M., Murphy, C., Wang, H.T., Hymers, M., Karapanagiotidis, T., Poerio, G., Margulies, D.S., Jefferies, E., Smallwood, J., 2018. Default mode network can support the level of detail in experience during active task states. Proc. Natl. Acad. Sci. USA 115, 9318–9323.
Sridharan, D., Levitin, D.J., Menon, V., 2008. A critical role for the right fronto-insular cortex in switching between central-executive and default-mode networks. Proc. Natl. Acad. Sci. 105, 12569–12574.
Stawarczyk, D., Majerus, S., Maquet, P., D'Argembeau, A., 2011. Neural Correlates of Ongoing Conscious Experience: both Task-Unrelatedness and Stimulus-Independence Are Related to Default Network Activity. PLoS One 6.
Uddin, L.Q., Menon, V., 2009. The anterior insula in autism: under-connected and under--examined. Neurosci. Biobehavioral Rev. 33, 1198–1203.
Ullsperger, M., Harsay, H.A., Wessel, J.R., Ridderinkhof, K.R., 2010. Conscious perception of errors and its relation to the anterior insula. Brain Structure Function 214, 629–643.
Vatansever, D., Menon, D.K., Stamatakis, E.A., 2017. Default mode contributions to automated information processing. Proc. Natl. Acad. Sci. 114, 12821–12826.
Wolff, M., Vann, S.D., 2019. The Cognitive Thalamus as a Gateway to Mental Representations. J. Neurosci. 39, 3–14.
Zeidman, P., Jafarian, A., Corbin, N., Seghier, M.L., Razi, A., Price, C.J., Friston, K.J., 2019. A guide to group effective connectivity analysis, part 1: first level analysis with DCM for fMRI. Neuroimage 200, 174–190.
Zhang, D., Snyder, A.Z., Shimony, J.S., Fox, M.D., Raichle, M.E., 2010. Noninvasive functional and structural connectivity mapping of the human thalamocortical system. Cereb. Cortex 20, 1187–1194.
Zhang, L., Luo, L., Zhou, Z., Xu, K., Zhang, L., Liu, X., Tan, X., Zhang, J., Ye, X., Gao, J., 2018a. Functional connectivity of anterior insula predicts recovery of patients with disorders of consciousness. Front Neurol. 9, 1024.
Zhang, Z., Zhang, D., Wang, Z., Li, J., Lin, Y., Chang, S., Huang, R., Liu, M., 2018b. Intrinsic neural linkage between primary visual area and default mode network in human brain: evidence from visual mental imagery. Neuroscience 379, 13–21.